A Comparison of Two Optical Methods for Measuring Line Averages of Thermal Exchanges Above Warm Water Surfaces[1]

MARVIN L. WESELY

Radiological and Environmental Research Division, Argonne National Laboratory, Argonne, Ill. 60439

(Manuscript received 13 February 1976, in revised form 4 October 1976)

ABSTRACT

Line averages of the vertical transports of sensible and latent heats in the surface boundary layer are determined above a warm water surface by the use of two optical, line-of-sight, remote-sensing techniques. In one method, the amount of atmospherically-induced blurring of images is observed visually with the aid of a small portable astronomical telescope. The other method utilizes unaided observations of the formation of inferior mirages, in particular the heights of distant objects that appear to be partially hidden behind the mirage. In the present application above industrial cooling ponds, lines of sight are within 1 m of the water surface and 0.4 to 1.5 km in length. The evaluation of the heat fluxes also requires estimates of the surface friction velocity and the ratio of the sensible to latent heat fluxes, each of which can be obtained with sufficient accuracy over a warm water surface from relatively simple measurements of temperatures and wind speeds. The direct visual measurements are highly reproducible and, since the equipment is easily deployed in the field, the thermal performances of different sections of the same pond can be evaluated rapidly. Agreement within 10% is found between values of the heat fluxes estimated by these methods and those obtained from low-level bulk-aerodynamic procedures, but only if lines of sight are chosen to ensure that fetch is adequate, particularly for the mirage observations.

1. Introduction

Sensible and latent heat fluxes in the surface boundary layer frequently are estimated with *in situ* methods which, because of the intermittent characteristics of turbulent flow, require either long-time averages at a single point or observations at multiple sites. Such requirements do not arise when remote sensing techniques that quickly yield spatial averages are used. In this paper, two optical line-of-sight remote-sensing methods for rapidly obtaining line averages of thermal exchanges above warm water surfaces are compared. The fluxes are determined indirectly and, in the present schemes, some simple *in situ* measurements are required. The experiment was performed over an industrial cooling pond where large amounts of heat and water vapor were transferred to the atmosphere, causing drastic optical effects.

In the optical method to be referred to as the "blurring" or "resolution" technique, line averages of thermal exchanges between the air and a cooling pond are inferred from observations of atmospherically-induced blurring apparent to the human eye (Wesely and Derzko, 1975). Fig. 1 shows an example of severe blurring. The atmospheric variable obtained is the refractive-index structure-function coefficient C_n^2, which can be related to the temperature and water vapor pressure parameters, C_T^2 and C_e^2, respectively (Wesely, 1976). These parameters can be used to estimate the sensible heat flux H and latent flux L_wE, provided some measure of the intensity of mechanical turbulence is obtained independently (e.g., Wyngaard *et al.*, 1971; Wesely and Alcaraz, 1973).

The second optical method to be considered is the "masking" or "mirage" technique, in which the extent of formation of an inferior mirage, caused by mean temperature and humidity gradients above the surface (Johnson, 1954), is measured. Fig. 1 shows such a mirage, especially on the right-hand side of the photograph where a 2 m high dike is nearly hidden behind a somewhat distorted reflection of the trees above the dike. Similar photographs can be found in recent publications (Friend and Stearns, 1970; Fraser, 1975). Measurements required for application of the masking technique are the "mirage height," which is the height of the observer above the water when a distant object is partially obscured, and the height of the object. (Because of the reciprocal nature of light-ray propagation, the height determined at either end of the line of sight can, in principle, be chosen to be called the "mirage height.") It has been shown by Stearns and Wesely (1974) that the mirage height is uniquely determined by the heat fluxes, friction velocity, line-of-sight distance, and the height of the object viewed.

In both optical methods, the information used to calculate heat fluxes is obtained by simple visual

[1] This work was supported by the U. S. Energy Research and Development Administration.

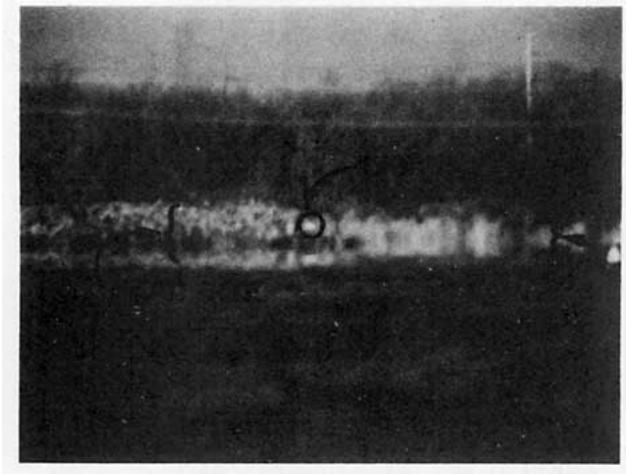

FIG. 1. Example of image blurring and mirage formation as viewed with a 12.7 cm diameter Cassegranian telescope with a magnification of 25×. The telescope is 0.92 m above the water surface at the southeast end of the path identified by D in Fig. 2, while the lights, identified by the circle and arrow in the photograph, are the same height at the opposite end of line D. On the right-hand side and 1600 m away is a 2 m high dike that is nearly hidden behind the mirage. Bulk measurements indicate that $H \approx 95$ W m^{-2}, $L_wE \approx 250$ W m^{-2} and $u_* \approx 0.17$ m s^{-1}.

observations (described in detail in Appendix A) that are sometimes along nearly the same line of sight. The two approaches are nevertheless quite different since the effects of mean gradients are seen in a mirage, while high-frequency fluctuations cause the appearance of blurring.

2. Analysis of image blurring

Although measurements can be obtained over any surface that is suitably flat and homogeneous, the discussion here is confined to propagation paths over warm water. A list of symbols and the values of some constants appear in Appendix B.

a. An equation for blurring in the atmosphere

The lengthy theoretical development necessary to show the relation between the limiting optical resolution of the atmosphere and C_n^2 will not be given here, as the present purpose is to emphasize the practical application of the procedure. The relationships that form the basis of the observed optical method are summarized by Wesely and Derzko (1974). It suffices to say that the variables necessary to determine C_n^2 include the limited-resolution distance d, the path length l, and the wavelength of light λ. We take for granted that the height of the propagation path is very nearly constant all along its length. A white light source is usually used, and while visible light of almost all wavelengths is ordinarily present, we can assume $\lambda = 0.55$ μm since this is the wavelength to which the human eye responds most efficiently.

As shown by Wesely and Derzko, a simple, empirical equation relating C_n^2 to the measured quantities can be used, provided the telescope's diameter D is greater than $4\lambda l/d$. Above the surface of a cooling pond where fluctuations in temperature and moisture content are both large, values of d are large; therefore, for the path lengths of several hundred meters usually available, the use of a telescope with $D > 10$ cm satisfies this requirement. However, if a telescope of a diameter much greater than 20 cm were used, the effects of larger scale fluctuations would be included. As a result, the apparent image position changes might appear slowed to the extent that some are seen by the eye as image dancing rather than blurring and C_n^2 would be underestimated.

With $D \approx 15$ cm the theory gives the simple formula

$$C_n = 0.44 d^{5/6} \lambda^{1/6} l^{-4/3}. \quad (1)$$

Note that there are no temperature, pressure, or stability influences explicitly included in this equation; these effects are taken into account in the expressions that relate C_n to the heat fluxes.

b. Equations relating C_n to heat fluxes

Above cooling ponds, both L_wE and H figure significantly in the total loss of heat from the pond. Here we shall determine the separate contributions of C_e and C_T to C_n and then use C_e and C_T to obtain the latent and sensible heat fluxes.

The theoretical background needed to develop equations that allow the calculations of C_e and C_T from C_n is given by Wesely (1976). The results of this analysis indicate that

$$C_e = C_n T / [(A_1 - A_2)\alpha_1], \quad (2)$$

$$C_T = C_n T^2 / (A_1 p \alpha_2), \quad (3)$$

where the A's are constants and the α's provide the means of partitioning the value of C_n into the magnitudes of C_e and C_T.

The form of the expressions for α_1 and α_2 depends on whether the fluctuations of temperature and humidity are correlated in the inertial subrange. It has been argued that close to the surface of a warm water surface, it is likely that temperature and water vapor pressure fluctuations are highly correlated (e.g., Wesely and Alcaraz, 1973; Friehe *et al.*, 1975), but recent measurements at the Dresden cooling pond show that this is only true of the low-frequency, flux-carrying eddies. With the use of a Lyman-α hygrometer and a 2 μm diameter fine-wire resistance thermometer about 1 m above the water surface at the Dresden cooling pond, a correlation coefficient R_{eT} between the two signals was measured for fluctuations remaining after passage through high-pass filters employing a variable time constant τ. The following empirical relationship was found:

$$R_{eT} \approx 0.95 \exp[-z(75\tau\bar{u})^{-1}]. \quad (4)$$

For a telescope with a 15.24 cm diameter lens, as was primarily used at the Dresden cooling pond, this results in an effective correlation coefficient of $r_{eT} \approx 0.25$ (a manuscript describing this analysis will be published elsewhere). This result can be used in the expressions (Wesely, 1976)

$$\alpha_1 = [1 + 2r_{eT}b_1\beta + (b_1\beta)^2]^{\frac{1}{2}}, \quad (5)$$

$$\alpha_2 = [1 + 2r_{eT}(b_1\beta)^{-1} + (b_1\beta)^{-2}]^{\frac{1}{2}}, \quad (6)$$

where

$$b_1 = \epsilon L_w (Tc_p)^{-1}(1 - A_2/A_1)^{-1}. \quad (7)$$

The magnitude of H can be calculated from the value of C_T when the height z above the surface and the friction velocity u_* are known, i.e.,

$$H = \rho c_p u_* C_T z^{\frac{1}{2}} S^{-1}, \quad (8)$$

where S is a dimensionless parameter that is an empirical function of stability (Wesely and Alcaraz, 1973). A procedure for determining u_* (and β) over water surfaces is given in Appendix A.

The value of L_wE can be determined from C_e, but the empirical functions and constants necessary to determine a stability dependency corresponding to S are not as precisely known for the case of moisture variables. However, micrometeorological evidence shows that temperature and specific humidity q do exhibit some similarities in transfer and turbulence characteristics. On this basis, we shall assume that at the same height $C_q/q_* = C_T/T_*$, which leads to the result

$$L_wE = \rho L_w u_* C_q z^{\frac{1}{2}} S^{-1}. \quad (9)$$

The approximation $C_q \approx \epsilon C_e/p$ gives

$$L_wE = \rho L_w u_* \epsilon C_e p^{-1} z^{\frac{1}{2}} S^{-1}. \quad (10)$$

The stability of the atmosphere can greatly affect the estimates of H and L_wE made with the foregoing relations. Thus, the stability parameter z/L should be evaluated accurately. The usual definition of z/L is

$$z/L = -kzgH(\rho c_p T u_*^3)^{-1}(1 + 0.61 c_p T L_w^{-1}\beta^{-1}). \quad (11)$$

Some of the details of the derivation of (11), including the "correction" term $(1 + 0.61 c_p T L_w^{-1}\beta^{-1})$ for moisture, are provided by Busch (1973). Since above cooling ponds $\beta \approx 0.1$, this term is necessary in the present application.

At a height of 1 m above a cooling pond, z/L is typically between -0.05 and -1.0. Within this range, the following empirical formula for the stability effects can be used:

$$S = 1 + 0.45(z/L + 1.5) + 0.01(z/L + 1.5)^{10}. \quad (12)$$

This gives S within $\pm 5\%$.

c. Calculation procedure

Substituting (1) and (2) into (10) and using the equation of state, we can show that

$$L_wE = 0.44\epsilon L_w u_* [R_a(A_1 - A_2)S\alpha_1]^{-1} d^{5/6}\lambda^{1/6} z^{\frac{1}{2}} l^{-4/3}. \quad (13)$$

TABLE 1. Summary of the formulas needed to calculate L_wE and H using visual observations of blurring and measurements of u_* and β. Case I is appropriate for summer conditions and case II for cold weather, but the effects of temperature on the numerical factors are evidently so small that their variations might be ignored in some applications. The values of L_wE and H are expressed in W m^{-2} and all other quantities are in SI base units. The value of $p = 100$ kPa is assumed.

$S = 1 + 0.45(z/L + 1.5) + 0.01(z/L + 1.5)^{10}$, $-1.0 < z/L < -0.05$

$L_wE = b_2 x 10^8 u_* d^{5/6} z^{1/3} l^{-4/3} S^{-1}\alpha_1^{-1}$

$H = b_3 x 10^6 u_* d^{5/6} z^{1/3} l^{-4/3} S^{-1}\alpha_2$

$\alpha_1 \approx [1 + 2r_{eT}b_1\beta + (b_1\beta)^2]^{1/2}$

$\alpha_2 \approx [1 + 2r_{eT}(b_1\beta)^{-1} + (b_1\beta)^{-2}]^{1/2}$

$r_{eT} \approx 0.95[1 - z(13D)^{-1}] \exp[-z(8.8D)^{-1}]$, $z < 13D$

$z/L = -1.1 \times 10^{-5} z H u_*^{-3}(1 + 0.07\beta^{-1})$

I. $T = 25°C$, $T_s = 30°C$:

$b_1 = 31$, $b_2 = 1.62$, $b_3 = 5.21$

(here revised to $b_2 = 1.78$ and $b_3 = 5.73$)

II. $T = 5°C$, $T_s = 10°C$:

$b_1 = 34$, $b_2 = 1.64$, $b_3 = 4.8$

(here revised to $b_2 = 1.80$ and $b_3 = 5.28$)

Similarly, by substituting (1) and (3) into (8), we can find that

$$H = 0.44 c_p u_* T(A_1 R_a S\alpha_2)^{-1} d^{5/6}\lambda^{1/6} z^{\frac{1}{2}} l^{-4/3}. \quad (14)$$

These formulas, together with (5) and (6) for the partition factors plus (11) and (12) for stability corrections, are the basis of the optical method calculation procedure. With use of appropriate values for constants and temperatures, the formulas summarized in Table 1 can be derived. Fortunately, the net temperature dependencies of the numerical terms in these equations are not great; therefore, precise measures of T and T_s are not required to determine the numerical factors.

During the period over which u_* and β are being averaged, the optical resolution distance d should be measured. With knowledge of the values of l, z, T and p, the following calculation procedure then can be used:

1) Estimate S based on a representative value of z/L. A value of S corresponding to z/L from -0.05 to -1.0 can be chosen. Typically at 1 m cooling ponds, $z/L \approx -0.1$, which results in $S \approx 1.9$.

2) Use (6) or a corresponding formula in Table 1, together with an estimate of r_{eT}, to obtain α_2. Since β is usually greater than 0.1, the use of the value $\alpha_2 = 1$ will result in less than 5% errors in the estimate of H.

3) Estimate H using (14) or the corresponding equation in Table 1. The value of L_wE can be obtained in a similar fashion, or simply by applying the relation $L_wE = H/\beta$.

4) Using the estimates of H or L_wE obtained in 3), calculate an improved value of z/L from (11) or the equivalent equation in Table 1 and use the new value to reestimate S with (12).

5) Repeat steps 3) and 4) until successive estimates of $(H+L_wE)$ do not change by more than about 1%. With a reasonable initial estimate of z/L only three or four iterations are usually necessary.

3. Analysis of masking by mirages

The calculation of sensible heat flux H and latent heat flux L_wE from the mirage height can be accomplished by use of the numerical techniques described by Stearns and Wesely (1974), in a scheme of successive approximations. With use of the measured values of the height z_1 of the viewed object, the line-of-sight distance l, β and u_*, the value of H (or L_wE) is repeatedly estimated until the observed value of the mirage height z_m is obtained. To avoid lengthy repetition, the details of the numerical techniques will not be given here. The complexity of the procedure is compounded by the necessity for rays with several different launch angles to be traced in each iteration, in order to find the ray that is closest to the surface at the other end of the path. Usually, it suffices to consider 0.1 mrad steps from about -0.5 to -2 mrad to find the minimum height. It should be noted that because of the reciprocal nature of light-ray propagation, it does not matter whether the numerical tracing is performed from light to observer or vice versa.

Two improvements can be made in the analysis given by Stearns and Wesely in order to obtain results that are more realistic. The first concerns their assumption that K_H/K_M, the ratio of the eddy diffusivity for heat to that for momentum, is unity for unstable conditions. Clearly, this emphasizes the image distortion predicted by some of the calculations given by Stearns and Wesely; however numerous tests in the present study

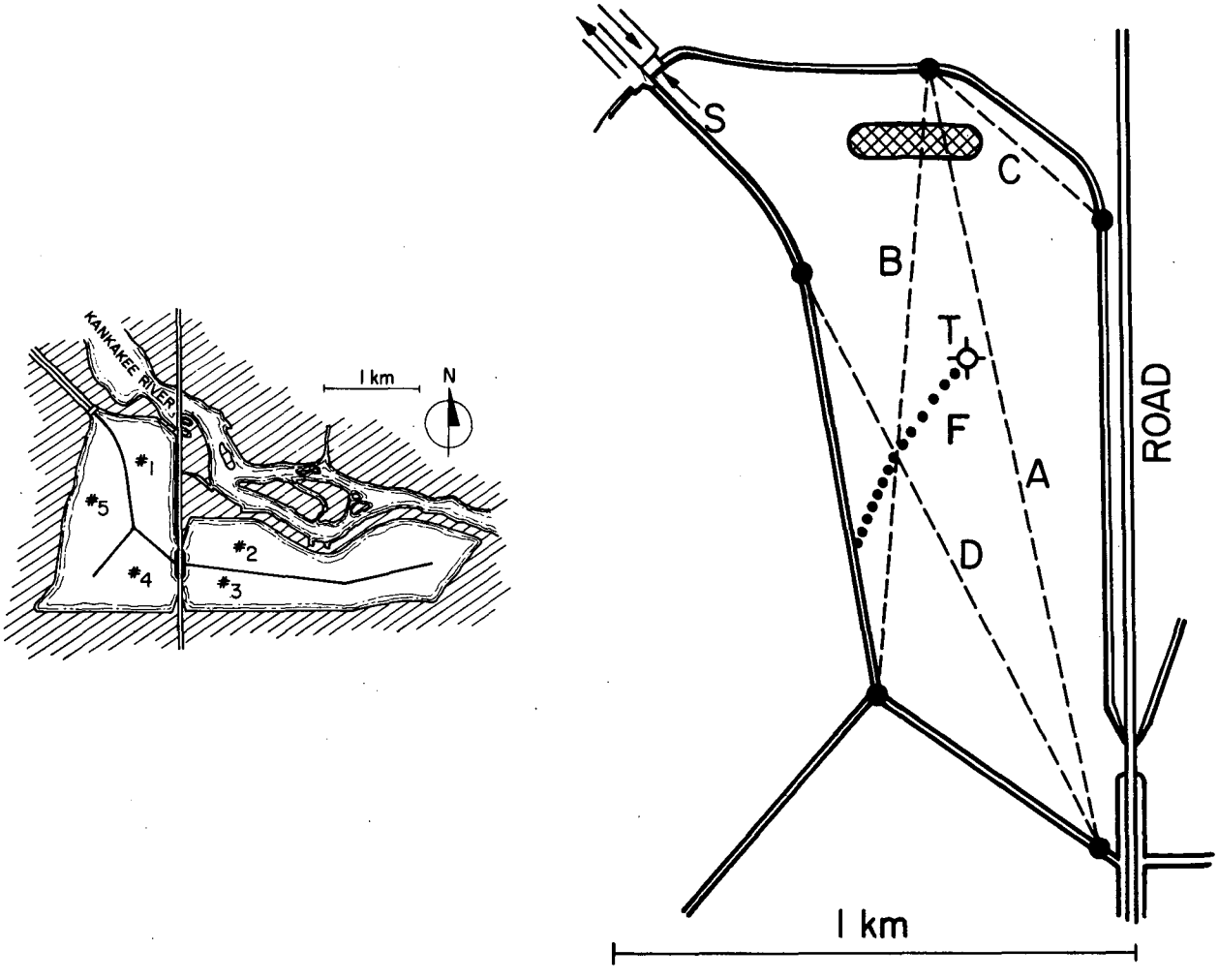

FIG. 2. Layout of the cooling pond for the Dresden nuclear power station. The warm water enters the complex via the lift station at S and circulates through Pools 1–5 sequentially. In the detailed drawing of Pool 1, the dashed lines A, B, C and D represent lines of sight employed for optical observations and the cross-hatched area indicates where the bulk measurements were taken in 1973. A stationary platform with a meteorological mast is located at T and the dotted line F represents the path traversed in a case study of spatial nonhomogeneity.

TABLE 2. Summary of heat fluxes measured above Pool 1. The identification of path line (of sight) refers to the dashed lines drawn in Fig. 2; winds were from the south or southwest when lines A and B were used and southeast when line C was used. Winds were easterly when line D was used, resulting in inadequate fetch for all the line averages. The point determinations were made by application of a low-level bulk-aerodynamic techniques (Hicks, 1975) to 15 min of temperature and wind measurements at points with fetch-to-height ratios of at least 400. All heat flux units are W m^{-2}.

Date	Time (CST)	Path Length (m)	Line	Point H	Point L_wE	Line average Blurring H	Line average Blurring L_wE	Line average Mirage H	Line average Mirage L_wE
Sept. 19–73	1515	1500	A	104	470	108	476	—	—
19–73	1605	1500	A	105	460	98	374	—	—
24–73	1342	1160	B	52	495	58	530	—	—
24–73	1427	1160	B	39	411	45	452	—	—
24–73	1506	1160	B	40	465	47	512	—	—
24–73	1537	1160	B	43	495	48	531	—	—
Oct. 3–73	1652	1500	A	63	430	57	361	42	280
3–73	1821	1500	A	91	439	79	397	57	302
3–73	1900	1500	A	92	439	74	365	63	325
3–73	1900	400	C	92	439	67	325	*	*
3–73	2001	1500	A	111	542	110	534	81	413
3–73	2001	400	C	111	542	92	444	*	*
5–73	1747	1500	A	78	393	66	323	54	280
5–73	1830	1500	A	67	319	43	199	39	192
5–73	1830	400	C	67	319	43	202	*	*
9–73	1215	1500	A	40	361	32	269	—	—
9–73	1310	1500	A	25	349	30	385	25	342
9–73	1352	1500	A	29	377	31	367	25	316
9–73	1430	1500	A	24	361	22	392	21	323
9–73	1507	1500	A	18	346	21	388	18	333
9–73	1544	1500	A	19	311	18	261	17	262
July 11–74	1338	1240	D	129	848	83	514	76	475
11–74	1358	1240	D	135	887	91	577	85	534
11–74	1418	1240	D	130	912	93	623	83	557
11–74	1438	1240	D	122	885	91	628	78	538
11–74	1458	1240	D	143	976	92	600	84	549
11–74	1608	1240	D	138	994	73	505	77	535
11–74	1628	1240	D	127	923	80	557	76	528
11–74	1648	1240	D	128	970	85	616	82	547
11–74	1708	1240	D	141	983	97	650	82	547
11–74	1728	1240	D	183	1199	110	693	89	556
11–74	1748	1240	D	157	990	96	573	91	545

* Mirage not present.

indicate that a significant improvement can be obtained using

$$K_H/K_M = 1/\phi_M, \tag{15}$$

where ϕ_M is the nondimensional wind-shear function (e.g., Dyer and Hicks, 1970). Of the nearly-equivalent empirical forms of ϕ_M for unstable conditions, the one recommended by Dyer (1974) is used here, i.e.,

$$\phi_M = (1-16z/L)^{-\frac{1}{4}}, \tag{16}$$

where z is the height of the ray.

The second improvement of the analysis given by Stearns and Wesely is that the numerical factor equal to A_1pT^{-2} in their Eq. (6) must be altered according to the actual values of mean temperature T rather than an arbitrary value representative of environmental temperatures. For the ray-tracing applications of interest here, measurements of T near the heights of the lights usually indicate that $A_1pT^{-2} \approx 0.88$. As a further refinement, the value of T for the height at each finite step along the ray path is recomputed from derived temperature gradients, and adjustments are made to take into account the rather substantial effect of water vapor gradients on the local refractive index gradients.

A final adjustment to the equations offered by Stearns and Wesely is that the stability parameter is modified to include the effects of water vapor on buoyancy, as shown earlier in (11).

4. Results

a. Site of the experiments

Measurements for the present study were taken over a moderately large cooling pond associated with the Dresden nuclear power station, operated by the Commonwealth Edison Company and located about 90 km southwest of Chicago. As shown in Fig. 2, this

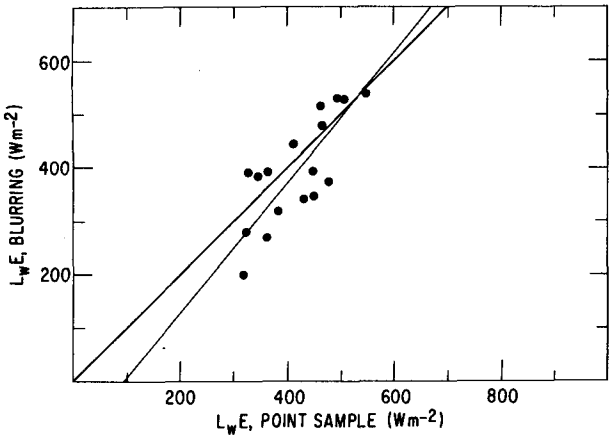

FIG. 3. Comparison of the latent heat fluxes determined by the image-blurring method with those measured using the low-level bulk-aerodynamic technique (point sample). The data, all taken from Table 2, are for the 1160 and 1500 m paths used during conditions of "good" fetch in 1973. The dark line is at 45° and the light line represents a linear regression with slope 1.21 ± 0.20 and intercept -108 W m^{-2}.

pond is divided into five segments, of which Pool 1 is the hottest and thus provides the best opportunity for study of the severe image blurring and masking by mirages found when the latent and sensible heat fluxes are large. Further, Pool 1 appears to be well mixed, since on several occasions surface water temperatures were found to be nearly uniform over the entire surface of the pool. Consequently, nonhomogeneities of this surface were assumed to be negligible. The optical data reported here are for lines of sight extending from shore to shore. Temperatures and winds were measured from a pontoon boat near a downwind portion of the propagation path, or from a stationary platform roughly in the center of Pool 1, at point T in Fig. 2.

b. Heat fluxes from image blurring

During September and October 1973, line averages of C_n were estimated by use of the image-blurring technique in a series of careful experiments over warm water; surface temperatures were about 30°C and air temperatures were about 25°C. As shown at A, B, and C in Fig. 2, propagation paths of 1500, 1150, and 400 m in length were used, each of these about 1 m above the water surface. Winds were from the southwest, south, and southeast during the experiments. Thus, fetches of more than 400 m existed all along the paths except near the south end of the pond where the light sources were located. Since the values of C_n obtained from the optical measurements are weighted toward the part of the optical path nearer the telescope, the effects of atypical C_n that may have existed in the initial part of the two long propagation paths were probably insignificant. Point measurements taken to determine u_* and β were obtained from the pontoon boat located as indicated by the cross-hatched area in Fig. 2, so that there was at least 1 km of uniform fetch over water.

At Dresden, light sources 1 m above the water surface and 1500 m away disappeared behind the mirage when observed from heights ranging from 0.25 to 0.75 m, depending on the conditions during observations. With optical paths of 400 m, these mirage heights were always less than 0.40 m. It follows from application of the criteria given in Appendix A that path heights of 1.0 and 0.8 m for the long and short paths, respectively, were about the minimum elevations that could be used without corrections for mean ray bending.

Some of the measurements of heat fluxes obtained during 1973 over the Dresden cooling pond are shown in Table 2. The low-level bulk-aerodynamic estimates of latent and sensible heat fluxes near the pontoon boat were determined in the manner described by Hicks (1975). Since these estimates are based on the same measurements of winds and temperature that were used to determine u_* and β for application of the optical formulas, the values of H and L_wE given by the bulk aerodynamic procedure are not entirely independent of those obtained with the image-blurring procedure. However, values of C_n are determined independently by the two techniques. The appropriate comparison indicates good agreement (Wesely and Derzko, 1975); if a partial correlation (25%) between temperature and humidity fluctuations is assumed, values of C_n obtained via optical measurements appear to be too small by about 10%.

As shown in Fig. 3, when the 1973 data are used the point estimates of H and L_wE closely agree with the optically-derived estimates. As shown in Table 3, the latter appear too small by about 10%. Therefore, when representative measurements of u_* and β are obtained, heat fluxes above cooling ponds can be determined successfully from visual observations of image blurring. Furthermore, comparison of simultaneous optical results for 400 and 1500 m paths given in Table 2 indicates approximately the same values of heat fluxes for the two different lines of sight. Evidently, the technique is sufficiently versatile to allow for a choice of path lengths suitable for most situations.

TABLE 3. A comparison of latent heat fluxes estimated using the present techniques. For 1973, the data are obtained from the eleven samples shown in Table 2 that correspond to when all three methods produced results. Also, the values for the 1974 data analyzed here are all shown in Table 2. The uncertainties are the standard errors.

	1973	1974
Resolution/bulk	0.909 ± 0.059	0.618 ± 0.031
Mirage/bulk	0.780 ± 0.055	0.561 ± 0.025
Mirage/resolution	0.852 ± 0.030	0.908 ± 0.024

c. Heat fluxes from masking by mirages

The numerical scheme for predicting the mirage height was tested with a series of measurements of mirage height z_m above Pool 1. Lights were placed 0.5 and 1.0 m above the water surface at the southeast corner of the pond and the mirage heights for various path lengths were observed, with the results illustrated in Fig. 4. During the half hour or so that elapsed during the test, measurements at the stationary mast near the center of Pool 1 indicated that the water temperature, air temperature, humidity, wind speed, and wind direction were nearly steady. The wind was approximately from the north so that adequate fetch existed for almost all of each propagation path. From the point measurements, u_* and β were estimated as described in Appendix A and H and L_wE were calculated by use of the low-level bulk-aerodynamic formulations. The latter values were used to predict the mirage heights numerically, with the results that agree very well with the observed heights, as can be seen in Fig. 4.

Some of the measurements of L_wE obtained in 1973 are listed in Table 2 and are further compared in Fig. 5. Since for all three measurement schemes it is assumed that $H=\beta L_wE$, where β is determined by gradients, similar comparisons exist for measurements of H. There are obvious serious discrepancies between the masking results and those from the low-level bulk-aerodynamic computations, with the latter giving values of L_wE about 130% of the former on the average. These and other discrepancies are discussed in the next subsection.

The complexity of the mirage analysis procedure requires that numerical calculation be performed on a computer. When rough estimates are needed quickly, an empirical estimate based on the formulas given by

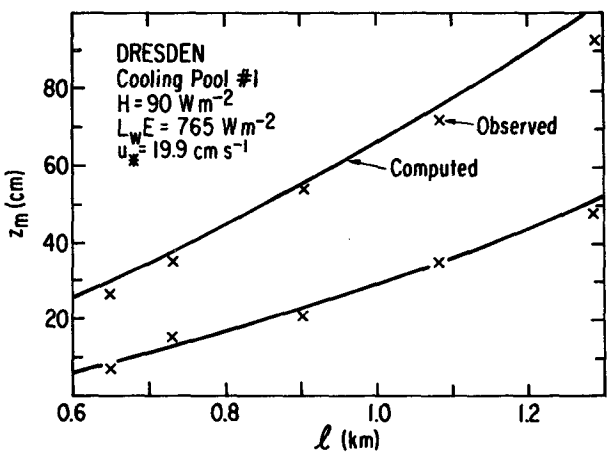

FIG. 4. Comparison between the observed mirage heights with those predicted by use of the numerical scheme. The estimates of H and L_wE were obtained by application of the low-level bulk-aerodynamic formulas, while u_* was determined based on a (assumed constant) drag coefficient and a wind speed at a height of 0.5 m.

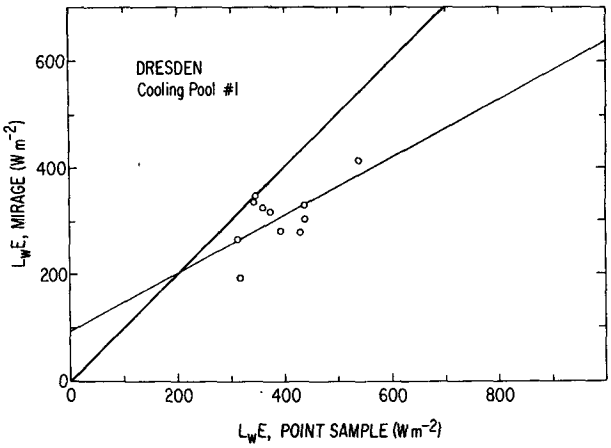

FIG. 5. Comparison between latent heat fluxes estimated from line-average mirage observations with those from bulk data. The data are taken from Table 2, when conditions of "good" fetch existed. The dark line is at 45° and the light line represents a linear regression with slope 0.53±0.21 and intercept 98 W m^{-2}.

Stearns and Wesely (1974) can be used. These show that z_1z_m/l^2 is approximately proportional to $L^{\frac{1}{2}}T_*$, which can be used to derive the result

$$H\approx 2.8\times 10^8(T/273)^2u_*^{\frac{1}{2}}z_1z_m[l^2(1+0.01/\beta)]^{-1}, \quad (17)$$

where all quantities are in SI base units. The numerical constant and the exponent of u_* were chosen for best agreement with the numerical results corresponding to the Dresden data. The factor $(1+0.01/\beta)^{-1}$ roughly takes into account the effects of water vapor content both on the buoyancy-induced production of mechanical turbulence and on the mean refractive index profile. This empirical solution provides estimates of H, and thus L_wE, that agree within 18% (one standard deviation) of the numerical results, with no detectable systematic variation with any of the parameters in the equation.

d. Effects of a change in surface properties upwind

As already mentioned, considerable care in choosing lines of sight was exercised during 1973 to make certain that adequate fetch existed along most of each propagation path. An analysis summarized in Table 3 indicates that the blurring estimates of the heat fluxes are about 10% less than the bulk results in 1973, and those obtained with the mirage estimates were on the average too small by more than 20%. It is suspected that the latter discrepancy is related to enhanced mixing caused by large, relatively strong, eddies immediately downwind of the dike bordering the subpond. This could have caused decreased temperature and humidity gradients near the south end of the line of sight. For the 1973 estimates based on observations of blurring, the fetch was adequate and this suggests that the numerical factor in (1), (3) and (14) is too small by 10%. Appropriate revisions have been suggested to the formulas in Table 1.

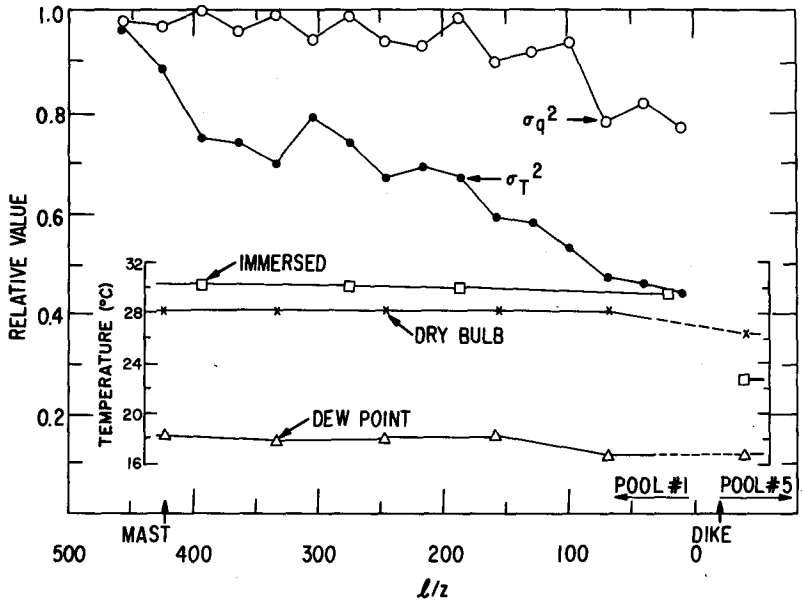

FIG. 6. A single-case set of measurements that show the effects of poor fetch on the magnitude of temperature and humidity fluctuations and mean values of dry-bulb, dew-point and water temperatures. The variances shown are actually ratios obtained by division by the magnitudes of the variances measured where the fetch-to-height ratio (l/z) exceeded 450. The bulk measurements show that in Pool 1 the values of the heat fluxes were $H \approx 38$ W m^{-2} and $L_wE \approx 604$ W m^{-2}, whereas upwind in Pool 5 they were $H \approx -78$ W m^{-2} and $L_wE \approx 284$ W m^{-2}.

To further illustrate the care required in choosing lines of sight, a sample of data collected on one day in 1974 is given in Table 2, for a case when path D in Fig. 2 was used. The pond was quite warm, about 39°C, and a cool east wind, at about 25°C near the upwind dike, was present. The heat fluxes appear extremely large (see Table 2), but it is not known to what extent the effects of the rather severe advection evidently present may have caused, by means of altering air temperatures and humidities, the estimates from application of the bulk formulas to be larger than the actual surface fluxes. Table 3 shows that both the resolution and the mirage methods give values of L_wE that are only about 60% of the bulk-method estimates. It is likely that both of the optical methods yielded underestimates because of poor fetch.

The absence of conclusive "standard" values of heat fluxes obtained for poor-fetch conditions during 1974 has led to more investigation. During October, 1975, direct measurements of the intensity of temperature and humidity fluctuations were obtained by real-time analog computations of variances of signals from a Lyman-α humidiometer and a fine-wire resistance thermometer. These devices, which had time responses less than 0.5 ms, were suspended 1 m above the water from a 2 m long boom oriented in the cross-wind direction from the pontoon boat. It can be shown that at this height and with the mean wind of about 6.7 m s^{-1} that prevailed, only the higher-frequency flux-carrying eddies were examined, since the variances σ_T^2 and σ_q^2 were computed after a removal of mean tends associated with a time constant of 0.07 s.

The pontoon boat was allowed to drift for about 15 min, from the dike at the south end of line F shown in Fig. 2 to slightly beyond the mast T. During this time, measurements of σ_T^2, σ_q^2, and the standard bulk measurements were taken, with the results shown in Fig. 6. A temperature inversion directly over Pool 5 probably was associated with the substantial reductions in σ_T^2 downwind in Pool 1. It is apparent that a fetch-to-height ratio of at least 400 is needed to avoid the effects of dissimilar surfaces upwind in such a situation. If we assume that σ_T^2 is directly related to C_T^2, then considerable underestimates in H and L_wE from (13) and (14) can result from poor fetch, whereas the bulk measurements (neglecting the minor reductions in wind speed near the dike) indicate that very little change in H and L_wE values would be calculated by use of the bulk formulations whenever the fetch-to-height ratio exceeds about 100. Hence, we conclude that improper use of the blurring technique *can* lead to serious errors in calculated values of H and L_wE, but that such large errors are not as likely to occur with the bulk technique.

5. Summary and conclusions

It has been shown that observations of both blurring of images and masking of images by mirages can be successfully used to determine the average sensible

and latent heat fluxes along lines of sight above the surface of a cooling pond. At about 1 m above the surface, path lengths varying from 400 to 1500 m are suitable for the blurring technique and paths at least 1000 m in length are usually needed for the mirage observations. Although the mirage heights are probably more easily observed than the limited-resolution angle, the evaluation of heat fluxes from measurements of mirage height involve more complex calculations, in the types of analyses suggested here.

Since the optical methods yield estimates of the vertical heat fluxes that are line averages, values of β and u_* that are determined at single points can be used only when appropriately representative values can be assured. Nevertheless, the optical techniques have the advantages of providing flux estimates that are fairly precise and that are obtained in a simple and reliable manner, so that it should be immediately obvious to an operator in the field whether or not measurements are correct. These advantages allow rapid assessment of the performance of different sections of a cooling pond by a procedure that should be considered as a feasible alternative to more conventional methods, which usually require the use of large amounts of equipment that is not very portable.

When a line of sight 1500 m in length and about 1 m above the surface is used, the blurring procedure with the lights placed at a discontinuity in surface roughness or energy balance (e.g., at a shoreline) can be successfully utilized, provided the lights are nearly directly upwind of the telescope used for observation. However, use of such a line of sight in the mirage method leads to H and L_wE being underestimated consistently by about 20% at the Dresden cooling pond. While use of the blurring method can be recommended with few reservations, precise quantitative measurements of heat fluxes using mirage observations are considerably more difficult to obtain. Unless a fetch-to-height ratio of about 400, say, can be ensured along *all* portions of the line of sight, the role of mirage observations in cooling-pond studies would be to obtain an exceedingly rapid, but inexact, impression of heat transfer.

The optical methods have the potential of being used over lines of sight considerably greater than the 1500 m maximum in the present study. If microwave and acoustic techniques for measuring the structure functions of humidity and wind along a line of sight (e.g., see Mandics *et al.*, 1973) can be developed for path lengths considerably greater than 100 m, then measurements of three structure functions near the same line of sight might provide estimates of line-averaged heat, water vapor, and momentum fluxes, without the use of point measurements. Over land surfaces it might be necessary to take measurements at 5–50 m above the surface to "smooth" the effects of local elevation changes, but over water surfaces, including the ocean, the main elevation concern is the effect of the curvature of the earth. Hence, line-of-sight measurements may have applications in meteorology where vertical fluxes averaged over large distances are desired. Conceivably, multiple slant paths could provide vertical flux profiles as well.

Acknowledgments. The work in this paper represents part of a team effort of the Atmospheric Physics Section, Argonne National Laboratory. The author wishes especially to thank Mr. B. B. Hicks, whose applications of the bulk formulations were essential to this study, and Mr. G. A. Zerbe, who assisted in the field work. The cooperation of the Commonwealth Edison Company in providing facilities at the Dresden cooling pond is appreciated, and Mr. M. J. Groppi of the Commonwealth Edison Company was particularly helpful in this regard.

APPENDIX A

Experimental Procedures

It is necessary to describe thoroughly the method of taking the optical measurements, since the observer's eyes are part of the optical system employed. It takes only one field trial to realize that standardized techniques must be applied in order to obtain repeatable results. Likewise, proper choices of locations for the lines of sight employed and for the *in situ* measurements are needed.

a. Image blurring

The measurement of C_n in the present scheme relies to some extent upon human judgment. The observer uses an astronomical telescope with a primary lens or mirror of about 15 cm diameter and at least 100× magnification; portable reflector or refractor telescopes commonly used by amateur astronomers are adequate. Two closely spaced point sources of light located at the far end of the selected line of sight are observed. When the observer is able to see two distinct point sources, closer spacings are successively presented until the observer decides that the sources appear as one. The process is then reversed until the light sources are barely discernible as two, and thus the desired separation distance is bracketed. With experience, an observer can quickly decide at what spacing the sources appear as neither one nor two point sources, but rather as one light source slightly elongated in one direction, with no indentations between the lights. These configurations are illustrated in Fig. 7. The critical separation distance d is recorded and the process is repeated during measurement of the average winds and temperatures that are required. Successive estimates of d ordinarily do not vary by more than 10%, and most of this variation is related to the intermittent nature of turbulent flow in the atmosphere.

Various schemes can be devised to produce the desired variable light source spacings. For optical

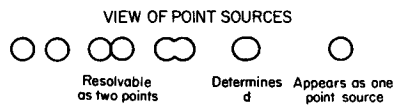

FIG. 7. The appearance of two point sources of light, blurred by the turbulent atmosphere, at various spacing when great magnification is used.

paths less than 500 m long at 1 to 2 m above the surface, where source separations are usually less than 5 cm, a single extended source of light can be placed behind masks with pairs of apertures manipulated by an assistant, controlled remotely, or moved continuously on a disk or wheel. Light sources particularly well suited include quartz-halogen lamps or mercury discharge lamps in tubular configurations. In order to keep the eye properly adjusted, a minimum light intensity should be used. Since the apparent brightness of the lights changes with the extent of blurring, it is desirable to use aperture diameters equal to about 10% of the critical distance d; alternatively, the light intensities should be adjusted for each spacing. Normally, a 200 to 300 W lamp (at least 6000 lumens) is needed during the daytime, but less intense sources should be used at night. For distances longer than 500 to 1000 m, the critical aperture spacings are usually greater than 5 cm and the use of two fully-exposed light bulbs is recommended. Quartz-halogen bulbs with a double-coiled, 1.5 cm long filament are sufficiently small and an autotransformer can be used to adjust lamp intensities for operation in various conditions of background lighting.

The height of the propagation path must be known. When a path several kilometers long is used, the earth's curvature will result in a variation of path height along the line of sight. This variation and its effects on the extent of observed blurring can be accounted for with a simple analytical expression. However, since ray bending caused by mean vertical refractive-index gradients has an additional effect on ray-path height that is difficult to determine, it is best to avoid the conditions of significant ray bending that can occur when an inferior mirage appears. For a "rule of thumb" concerning the minimum height that can be used with negligible errors in H and L_wE determined from C_n, we can refer to the numerical analyses performed by Stearns and Wesely (1974). With these results it can be shown that for path heights of 1–2 m about 10% overestimation in effective path height would result if the telescope height were twice as great as that at which the light sources just appear to be "extinguished" by the mirage. This is equivalent to only about a 3% overestimate in H and L_wE.

Prior to installation of the experimental apparatus at a cooling pond, the prevailing wind direction relative to the shape and orientation of the pond should be considered. The stations where equipment is located should be separated by at least 400 m and the telescope and the light sources, usually at shorelines, should be at the same height above the water surface. It is desirable that the line of sight be approximately normal to the mean wind, in order that all portions of the optical path have an adequate fetch-to-height ratio; a minimum value of this ratio is 100–400, depending on the characteristics of the surface upwind of the pond of interest. If sufficiently long fetches are not available for the entire path, the telescope should be placed in the downwind position where the better fetch conditions exist, since that portion of the path located nearest the light sources is the least significant in causing image blurring (Wesely and Derzko, 1975).

b. Masking by mirages

The mirage height can be determined across a known distance with a small light placed at some reasonable height above the surface. A telescope is not needed, although observation of dim light sources would be aided by the use of low-magnification devices. To determine the mirage height, the observer notes the height of his eye when the distant light appears to be barely "extinguished." The viewer then slowly raises his position and records the height of his eye when the source first seems to separate into an upper light and a lower light. The mirage height is taken to be the average of the two heights recorded, which usually differ by about 20%. This difference is associated with the rapid fluctuations of refractive index along the ray path. In order to keep this difference at a minimum, the eye should be kept properly adjusted by using the lowest light intensity that is adequate for observation.

For mirage observations above cooling ponds, the same care in choosing the location of the line of sight should be taken as is required for blurring measurements. Because of the limited fetch usually available, the heights of both the light source and the observer's eye should be less than 1 m above the pond. A good arrangement is to place one light at 0.5 m and another at 1.0 m above the water, usually at a shoreline; this configuration frequently results in a suitable mirage being found when viewed across a path about 1 km in length. In most cases, the positions of the ray path that are closest to the water surface have the most effect in determining the mirage height. Therefore, if the observation height is less than the height of the light when in the position of masking, it is desirable for the observer to be in the downwind location in order to minimize the effects of poor fetch.

c. Measurements of u_* and β

For determination of heat fluxes by use of either the blurring or the masking techniques, information on both the magnitude of mechanical mixing and the relative importance of temperature and humidity variations in causing refractive index changes is

required. The atmospheric variables involved are the surface friction velocity u_* and the Bowen ratio $\beta \equiv H/L_wE$. Point estimates of u_* and β can be obtained over water with relatively simple measurements, but these should be taken far enough away from shorelines to avoid limitations imposed by inadequate fetch and nonrepresentative water surface temperatures often found near the shore.

The friction velocity can be estimated above water with use of a "friction coefficient," that is, the square root of a drag coefficient (e.g., Priestley, 1959). Assuming the drag coefficient appropriate to winds measured at 10 m to be about 1.3×10^{-3}, we can use wind-profile relations to show that for the mean wind speed u at 1 m is

$$u_* \approx 0.045u. \tag{A1}$$

Although the value of the numerical coefficient in (A1) can lead to values of u_* that are too low by about 10% in the highly unstable conditions that frequently exist above cooling ponds, the final estimates of the heat fluxes are not significantly affected because of the nature of the diabatic corrections employed.

Assuming that the air in contact with the water is saturated with water vapor at the surface temperature, we can compute the mean-gradient Bowen ratio as follows:

$$\beta = \gamma(T_s - T_d)/(e_s - e), \tag{A2}$$

where γ is the psychrometric constant, e_s is the saturation vapor pressure corresponding to the surface temperature T_s, and e is the mean water vapor pressure of the air at the same height as the dry-bulb temperature T_d is obtained. Wet- and dry-bulb temperature measurements sufficiently accurate for computation of e can be obtained over warm water surfaces with an ordinary ventilated psychrometer of the Assmann type, but it is desirable to use an infrared thermometer to measure the actual temperature of the water surface.

APPENDIX B

List of Symbols

A_1 refractive index constant for dry air ($=7.87\times10^{-4}$ K kPa^{-1} for $\lambda=0.55$ μm)
A_2 refractive index constant for water vapor ($=6.63\times10^{-4}$ K kPa^{-1})
b_1 the factor $\epsilon L_w(Tc_p)^{-1}(1-A_2/A_1)^{-1}$
b_2 the factor $0.44\epsilon L_w[R_a(A_1-A_2)]^{-1}\lambda^{1/6}$
b_3 the factor $0.44c_pT(A_1R_a)^{-1}\lambda^{1/6}$
C_e^2 structure function coefficient for water vapor pressure
C_n^2 structure function coefficient for refractive index
C_q^2 structure function coefficient for specific humidity
C_T^2 structure function coefficient for temperature
c_p specific heat of air at constant pressure ($\sim$1019 J kg^{-1} K^{-1})
D diameter of telescope aperture
d distance between two light sources when just resolved
E evaporation rate; vertical mass flux of water vapor
e water vapor pressure
e_s mean water vapor pressure for saturated air at T_s
g acceleration due to gravity ($=9.8$ m s^{-2})
H vertical flux of sensible heat
K_H eddy diffusivity for heat
K_M eddy diffusivity for momentum
k von Kármán constant ($\sim$0.4)
L Obukhov scale length for the atmospheric surface layer
L_w latent heat of vaporization of water ($\sim2.56\times10^6$ J kg^{-1})
l length of a horizontal linear line
n refractive index of air
p static atmospheric pressure
q specific humidity
q_* specific humidity scaling parameter $[E/(\rho u_*)]$ in the atmospheric surface layer
R_a gas constant for dry air ($=287$ J kg^{-1} K^{-1})
R_{eT} integral correlation coefficient for e and T
r_{eT} spectral correlation coefficient for e and T
S stability factor $(C_T z^{\frac{1}{2}}/T_*)$ for propagation path
T_d dry bulb temperature
T_s temperature of water surface
T_* temperature scaling parameter $[H/(\rho c_p u_*)]$ in the atmospheric surface layer
u mean horizontal wind speed
u_* surface friction velocity
z height above the water surface
z_m height of observer when object viewed is just obscured by a mirage
z_1 height of object viewed when just obscured by a mirage
α_1 factor for finding C_e from C_n; see (5)
α_2 factor for finding C_T from C_n; see (6)
β Bowen ratio (H/L_wE)
γ psychrometric constant $[pc_p/(\epsilon L_w)]$; $\sim$0.066 kPa K^{-1}
ϵ ratio of molecular weight of water to that of air ($=0.622$)
λ wavelength of light
ρ air density ($\sim$1.2 kg m^{-3})
σ_T^2 variance of temperature
σ_q^2 variance of specific humidity
ϕ_M nondimensional wind-shear function

REFERENCES

Busch, N. E., 1973: On the mechanics of atmospheric turbulence. *Workshop on Micrometeorology*, D. A. Haugen, Ed., Amer. Meteor. Soc., 1–65.

Dyer, A. J., 1974: A review of flux-profile relationships. *Bound.-Layer Meteor.*, **7**, 363–372.

——, and B. B. Hicks, 1970: Flux-gradient relationships in the constant flux layer. *Quart. J. Roy. Meteor. Soc.*, **96**, 715–721.

Fraser, A. B., 1975: Theological optics. *Appl. Opt.*, **14**, A92–A93.

Friend, A. L., and C. R. Stearns, 1970: Improved method for the optical determination of temperature profiles. *Bound.-Layer Meteor.*, **1**, 227–239.

Friehe, C. A., J. C. La Rue, F. H. Champagne, C. H. Gibson and G. F. Dreyer, 1975: Effects of temperature and humidity fluctuations on the optical refractive index in the marine boundary layer. *J. Opt. Soc. Amer.*, **65**, 1502–1511.

Hicks, B. B., 1975: A procedure for the formulation of bulk transfer coefficients over water. *Bound.-Layer Meteor.*, **8**, 515–524.

Johnson, J. C., 1954: *Physical Meteorology*. The MIT Press, 343 pp.

Mandics, P. A., R. W. Lee and A. T. Waterman, Jr., 1973: Spectra of short-term fluctuations of line-of-sight signals: Electromagnetic and acoustic. *Radio Sci.*, **8**, 185–201.

Priestley, C. H. B., 1959: *Turbulent Transfer in the Lower Atmosphere*. The University of Chicago Press, 130 pp.

Stearns, C. R., and M. L. Wesely, 1974: Light refraction by mean temperature gradients in the near-earth atmosphere. *Bound.-Layer Meteor.*, **7**, 411–428.

Wesely, M. L. 1976: The combined effect of temperature and humidity fluctuations on refractive index. *J. Appl. Meteor.*, **15**, 43–49.

——, and E. C. Alcaraz, 1973: Diurnal cycles of the refractive index structure function coefficient. *J. Geophys. Res.*, **78**, 6224–6232.

——, and Z. I. Derzko, 1975: Atmospheric turbulence parameters from visual resolution. *Appl. Opt.*, **14**, 847–853.

Wyngaard, J. C., Y. Izumi and S. A. Collings, Jr., 1971: Behavior of the refractive index-structure parameter near the ground. *J. Opt. Soc. Amer.*, **61**, 1646–1650.